Eur. J. Mech. B - Fluids 19 (2000) 637–652

S0997-7546(00)00114-X/FLA

Low frequency sound generated by flow separation in a conical diffuser

Karl-Richard Fehse [1], Wolfgang Neise [2]

Deutsches Zentrum für Luft- und Raumfahrt e.V., Institut für Antriebstechnik Abteilung Turbulenzforschung, Müller-Breslau-Straße 8, 10623 Berlin, Germany

(Received 28 April 1999; revised 9 November 1999; accepted 27 December 1999)

Abstract – The sound field in a circular pipe generated by a concentric jet flow entering the pipe is studied. In the first case the air flow enters the pipe through a convergent nozzle only. In the second case a short diffuser is attached to the nozzle. When the diffuser half angle is small enough to ensure attached flow conditions, the sound pressure level in the duct is reduced over the entire frequency range measured. When the diffuser angle is increased up to the point where flow separation occurs, an increase in the duct sound pressure level is observed. It is shown by means of cross-correlation measurements involving the unsteady wall pressures in the diffuser and the sound pressure in the duct that the increased sound levels are in fact caused by the flow separation in the diffuser. © 2000 Éditions scientifiques et médicales Elsevier SAS

sound / generation / flow / separation / diffuser

Nomenclature

a	phase velocity
a_0	speed of sound
d	pipe diameter
d_{jet}	jet diameter
f	frequency
k	$= 2\pi/\lambda$; wave number
L_p	pressure level re 20 μPa
Ma_0	$= u_0/a_0$; jet exit flow Mach number
p	static flow pressure
P	sound power
R	$d/2 =$ pipe radius
Re	$= u_0\, d_{jet}/\nu$ Reynolds number
u	flow velocity
u_0	jet exit flow velocity
γ^2	coherence function
λ	sound wavelength

[1] Now at TRW Fahrwerksysteme GmbH & Co. KG, Hansaallee 190, 40547 Düsseldorf, Germany
[2] Correspondence and reprints; e-mail: Wolfgang.Neise@dlr.de

ν kinematic viscosity
ρ_0 air density
w $= 2\pi f$; angular frequency

1. Introduction

In an earlier paper Stahl and Argüello [1] investigated the sound field in a circular pipe generated by a concentric jet flow entering the pipe through a convergent nozzle; see the schematic of the experimental facility in *figure 1* and *figure 2*. The pipe diameter was $d = 100$ mm; different nozzle diameters were used in the study but only the case $d_{jet} = 30$ mm is considered here. In *figure 3* are shown wall pressure spectra measured at an axial location eleven pipe diameters downstream of the exit plane of the nozzle $(x/d = 11)$. Three cases are compared: in the first the air flow enters the pipe through the convergent nozzle only; in the second a short diffuser of length $L = d$ and wall angle $\varepsilon = 3°$ is attached to the nozzle, and in the third the diffuser half angle is increased to $\varepsilon = 7°$. In all three cases the mass flow entering the pipe is kept constant; the flow Mach number in the nozzle constriction is $Ma_0 = u_0/a_0 = 0.3$.

Addition of a diffuser lowers the velocity of the jet flow entering the pipe, and as result the sound pressure level in the duct is reduced. In the case of the smaller diffuser angle $\varepsilon = 3°$, this is true for the entire frequency range measured, whereas for the diffuser angle $\varepsilon = 7°$ an increase in sound pressure level of as much as 15 dB

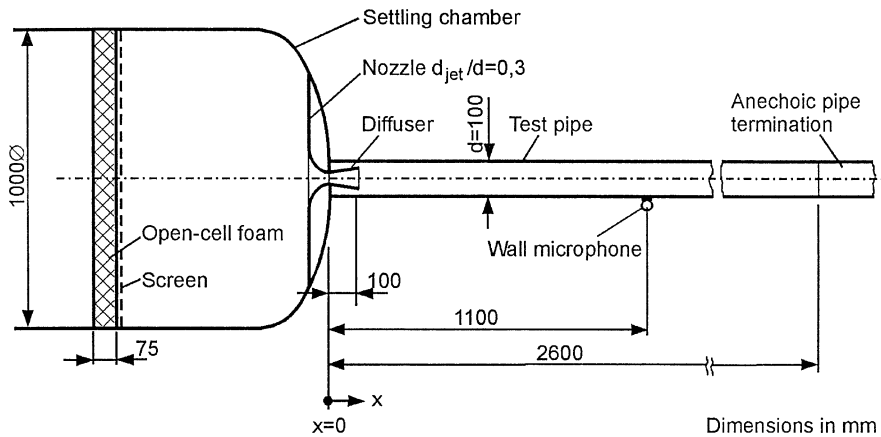

Figure 1. Schematic of the experimental rig used by Stahl and Argüello [1] and in the present study.

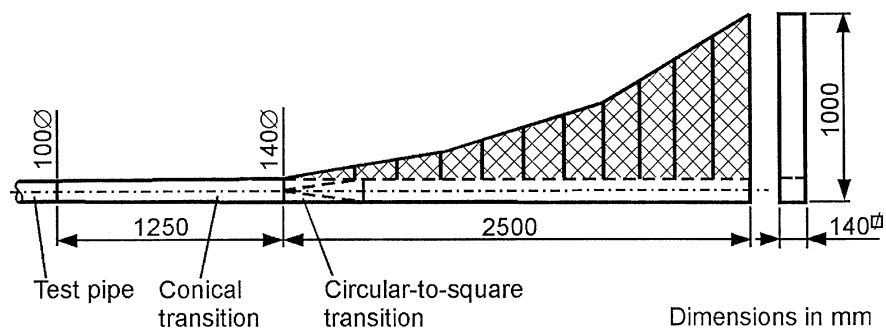

Figure 2. Schematic of the anechoic pipe termination.

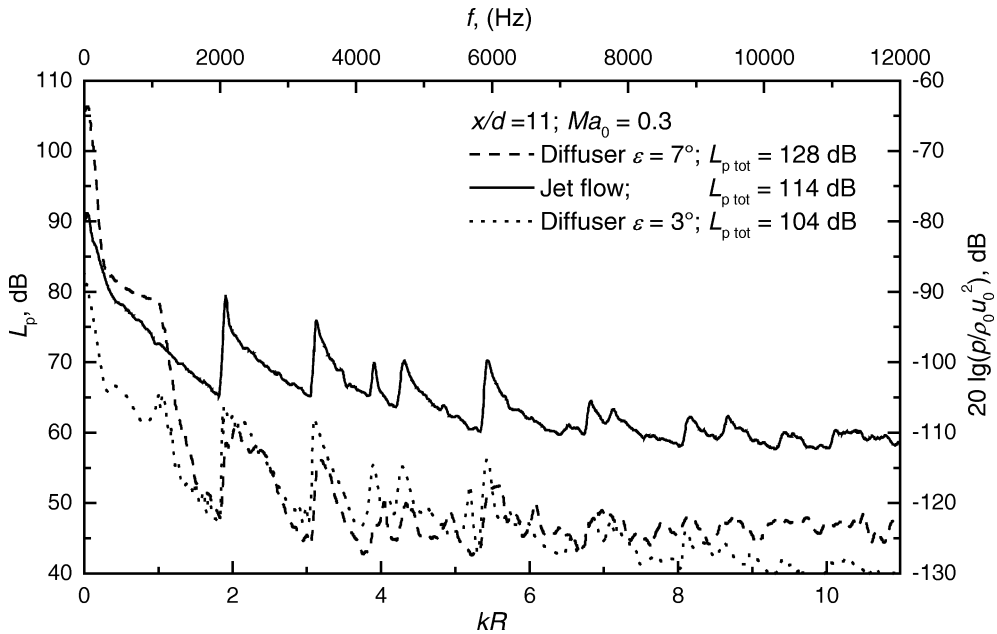

Figure 3. Wall pressure spectra in a circular pipe generated by a concentric jet flow (after Stahl and Argüello, [1]).

compared to the nozzle only spectrum is observed at frequencies below 1200 Hz. According to the results of many experimental studies, which were summarised by Klein [2], flow separation occurs in the 7°-diffuser but not in the 3°-diffuser. This is a clear hint that the low frequency level increases are caused by the separated flow in the 7°-diffuser.

In the present paper the above effect is studied further by applying cross-correlation analyses to the wall pressures in the diffusers and the sound field in the subsequent pipe.

2. Experimental apparatus

The experimental rig used is practically the same as in the study of Stahl and Argüello [1]. The flow delivered by a silenced centrifugal compressor is blown into a settling chamber of 1000 mm diameter equipped with a mesh screen and a 75 mm thick open-cell foam mat to provide uniform and turbulence-free flow conditions at the entrance of the circular convergent nozzle with exit diameter $d_{jet} = 30$ mm, see *figure 1*. $L = 100$ mm long diffusers of different expansion angles are mounted downstream of the nozzle. The diameter of the pipe into which the jet is discharged is $d = 100$ mm. The pipe is anechoically terminated (see the sketch in *figure 2*) to suppress axial acoustic resonances at frequencies above 50 Hz. The sound field in the pipe is monitored by using a 1/8-inch condenser microphone mounted flush with the inner pipe wall at an axial distance from the nozzle exit plane of eleven pipe diameters $(x/d = 11)$.

Sketches of the diffusers with the measurement locations for the wall pressures are depicted in *figure 4* and *figure 5*. To facilitate flow visualisation experiments, the diffusers consist of two lengthwise halves which are clamped together. The wall pressures in the diffusers are measured by using conventional pressure taps to which 1/4-inch condenser microphones are connected via a coupling device; see the schematic in *figure 6*. The change of the frequency response of a 1/4-inch microphone due to the pressure tap plus the coupler is plotted in *figure 7*. For more details see the theses by Cekici [3] and Fehse [4].

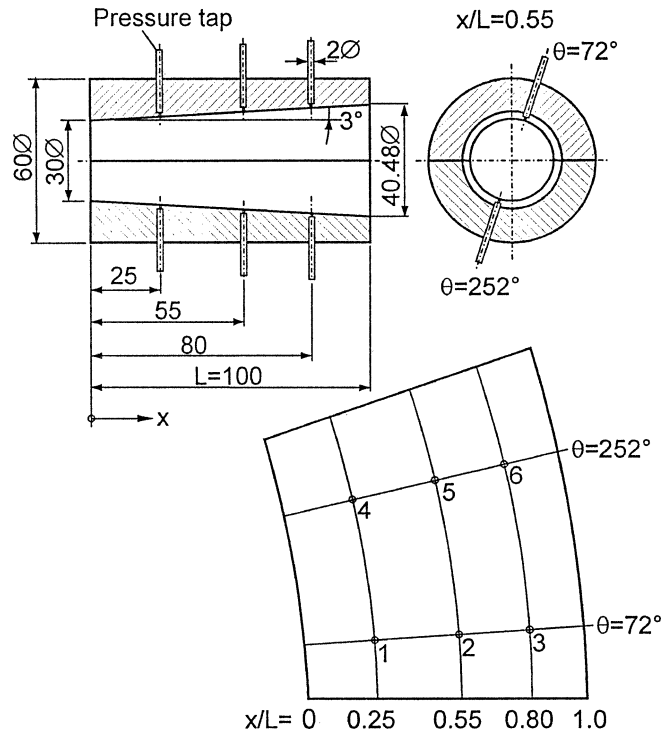

Figure 4. Sketch of the diffuser with half angle $\varepsilon = 3°$ with pressure measurement locations (dimensions in mm).

3. Experimental results

Experiments were made with only one flow condition which is characterised by the flow Mach number in the nozzle constriction $Ma_0 = 0.3$, the corresponding Reynolds number based on the nozzle diameter being $Re = u_0\, d_{jet}/\nu = 2 \times 10^5$. In the first step, the sound pressure spectra reported by Stahl and Argüello [1] were reproduced to make sure that the physical effect to be investigated is the same as in the earlier paper, see *figure 3*. Note that dimensional as well as non-dimensional coordinates are used in *figure 3*. The frequency range 0–12000 Hz corresponds to non-dimensional frequencies up to $kR = 11$. When the wall pressure levels are based on $\rho_0 u_0^2$ rather than on the usual acoustic reference pressure $p_0 = 20\ \mu$Pa, pressure levels become smaller by 170 dB. In the following figures, the conventional pressure levels and frequency scales are used for convenience.

The frequency range where only plane sound waves can propagate in the pipe ($d = 100$ mm) is from 0 to 2010 Hz ($kR = 0$ to 1.841). Beginning at that frequency, the onset of higher-order acoustic modes is clearly visible in the spectra for all three configurations measured. The total sound level in the duct is reduced from 114 to 104 dB when the 3°-diffuser is installed, and increased up to 128 dB in case of the 7°-diffuser. The level increase due to the 7°-diffuser is particularly strong at frequencies below 200 Hz ($kR < 0.18$). It is emphasized at this point that the sound levels produced by the separated shear layer along the diffuser wall are higher than the ones generated by the free shear layer of the jet flow emanating from the convergent nozzle.

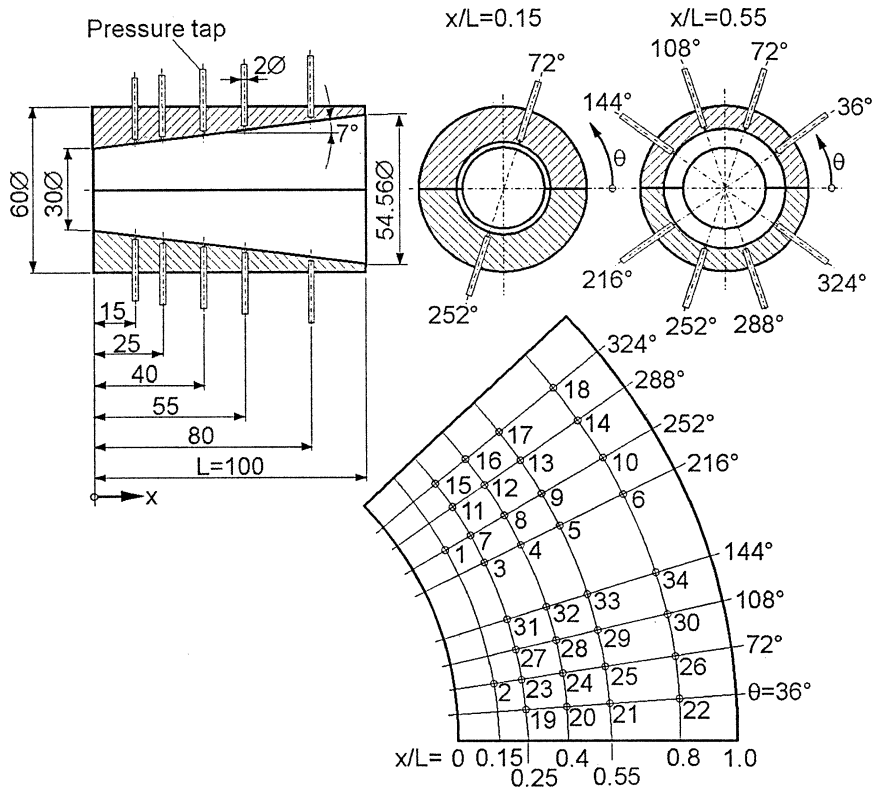

Figure 5. Sketch of the diffuser with half angle $\varepsilon = 7^\circ$ with pressure measurement locations (dimensions in mm).

3.1. Flow visualisation experiments

For this purpose the interior diffuser walls were covered with a self adhesive plastic sheet and painted with an oil-petroleum-soot-mixture. The flow was turned on until only the solid particles remained on the wall surfaces. Then the two diffuser halves were unbolted, and the plastic sheet peeled off the diffuser wall and unrolled to expose the image of the interior wall streamlines. The result of such experiments is shown in *figure 8*. In case of the 3°-diffuser, an entirely axisymmetric flow pattern is visible while in the case $\varepsilon = 7^\circ$ the flow pattern is non-axisymmetric and indicates flow separation occurring at about 15% of its total length. Careful experiments were performed to ensure that the asymmetric flow characteristic was not caused by any deviation from axisymmetry of the flow in the settling chamber or convergent nozzle. In fact, repeating the visualisation experiments several times revealed that the flow separation region did not occur at the same circumferential location but changed position randomly from test to test. Obviously, the experimental facility does not 'trigger' the onset of flow separation at a certain circumferential position, and hence the location of the separated flow regime is determined by random flow disturbances. It takes about 10 to 20 minutes before the oil-petroleum is evaporated and wall stream line patterns like the ones in *figure 8* are produced. There is a sharp border line between the flow separation and the main flow diverted around it. This indicates that the flow separation region is fairly stable in both size and position because any migration of it during 10–20 minutes 'averaging time' would result in a fuzzy border regime rather than a sharp line. A schematic presentation of the flow pattern in the 7°-diffuser constructed from the wall streamlines in *figure 8* is shown in *figure 9*. For more details see Fehse [4].

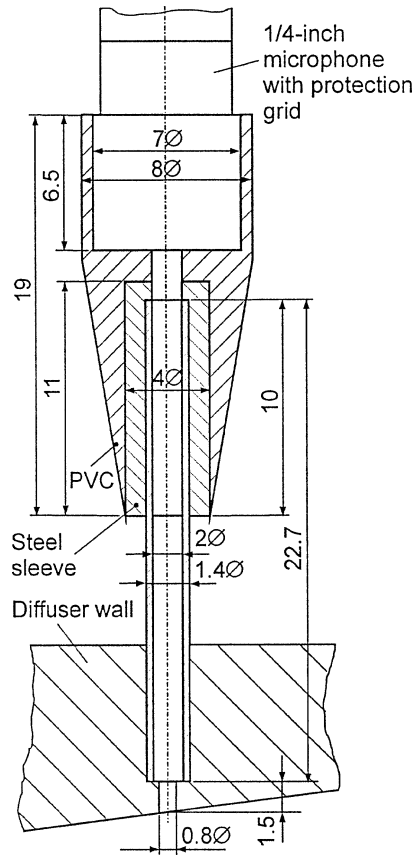

Figure 6. Schematic of a pressure tap in the diffuser wall connected to a 1/4-inch microphone via a coupling device (dimensions in mm).

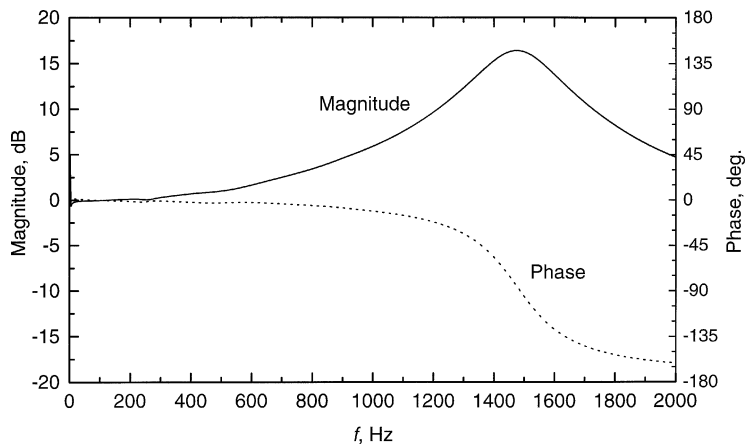

Figure 7. Frequency response of the pressure tap/coupler/1/4-inch microphone combination relative to a 1/4-inch microphone only.

3.2. Steady diffuser wall pressures

The static wall pressure p relative to that at the diffuser entrance p_1 and normalised by the theoretical pressure rise $(p_2 - p_1)_{theor} = \rho_0(u_1^2 - u_2^2)/2 = \rho_0 u_0^2[(d_2/d_1)^4 - 1]/2$ in both diffusers is plotted in *figure 10*. The

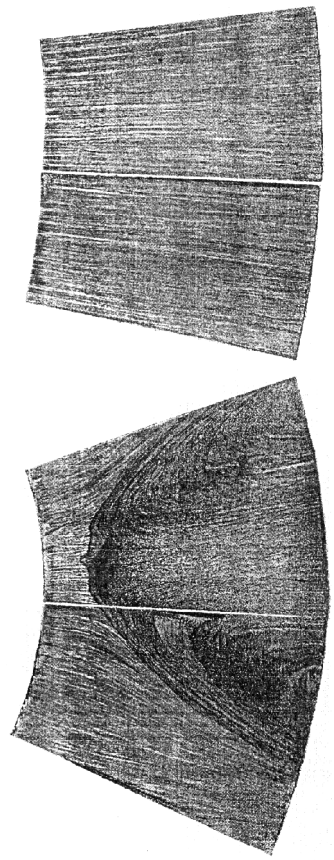

Figure 8. Wall streamlines in a conical diffuser ($Ma_0 = 0.3$); top: $\varepsilon = 3°$, bottom: $\varepsilon = 7°$.

subscripts 1 and 2 refer to entrance and exit of the diffusers. The local pressures p represent the circumferential average over all measurement positions at each axial location x/L. Near the entrance, the axial gradient of the relative static wall pressure is larger for the 7°-diffuser but levels off to become smaller than that of the 3°-diffuser near the exit which is of course the result of the flow separation in the former. At $x/L = 0.80$, the static pressure in the 3°-diffuser reaches 84% of the theoretical value, in the 7°-diffuser only 71%. The static wall pressure in the 3°-diffuser is axisymmetric but not so in the 7°-diffuser, compare the measurement results shown in *figure 11*. The average circumferential pressures for each axial distance from the diffuser entrance are indicated as horizontal lines.

Note that the results shown in *figure 10* and *figure 11* were obtained during one and the same experimental run during which the position of the flow separation area in the 7°-diffuser did not change.

3.3. Unsteady diffuser wall pressures

Spectra of the diffuser wall pressures are plotted in *figure 12*. The left column is for the 3°- diffuser and the right column for the 7°-diffuser. All spectra shown are corrected for the frequency response of the pressure tap/coupler combination plotted in *figure 7*. Results are shown for three axial planes of the former and for five axial planes of the latter; see the sketch of the measurement locations in *figure 4* and *figure 5*. All experimental results discussed in this section for the 7°-diffuser were obtained during one experimental run to ensure that

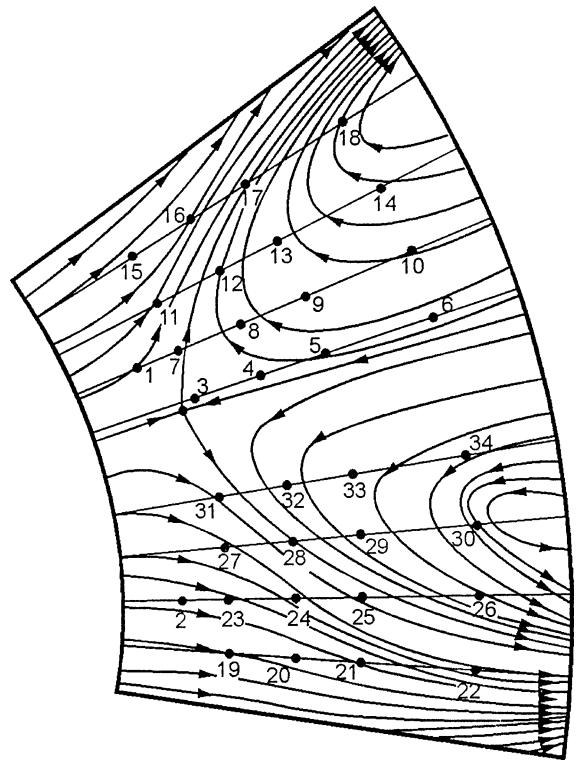

Figure 9. Schematic presentation of the wall streamlines in the 7°-diffuser ($Ma_0 = 0.3$).

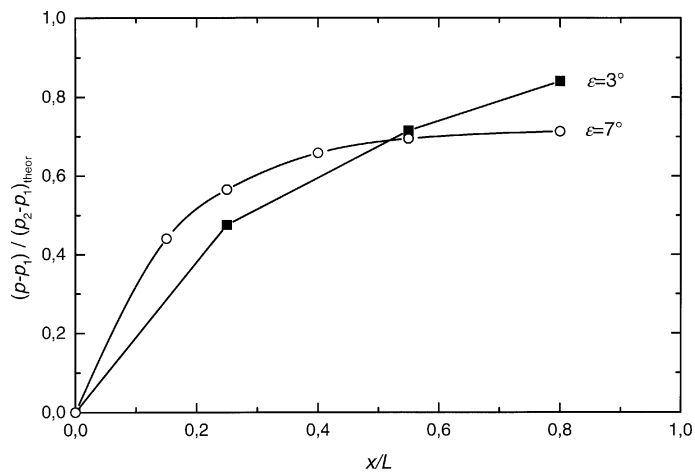

Figure 10. Streamwise variation of the static wall pressures in the 3°- and 7°-diffuser ($Ma_0 = 0.3$).

the experimental observations made are not obscured by a change in the position of the flow separation regime. While the wall pressure spectra in the 3°-diffuser are independent of the azimuthal angle, they differ by as much as 10 dB in the 7°-diffuser, depending on the axial distance from the nozzle exit and on frequency. Hence, the deviation from axisymmetry is much more pronounced in the unsteady wall pressures, 10 dB is equivalent to a factor of 3.16, than in the steady wall pressures where the deviation amounts to maximum 4%. Note that

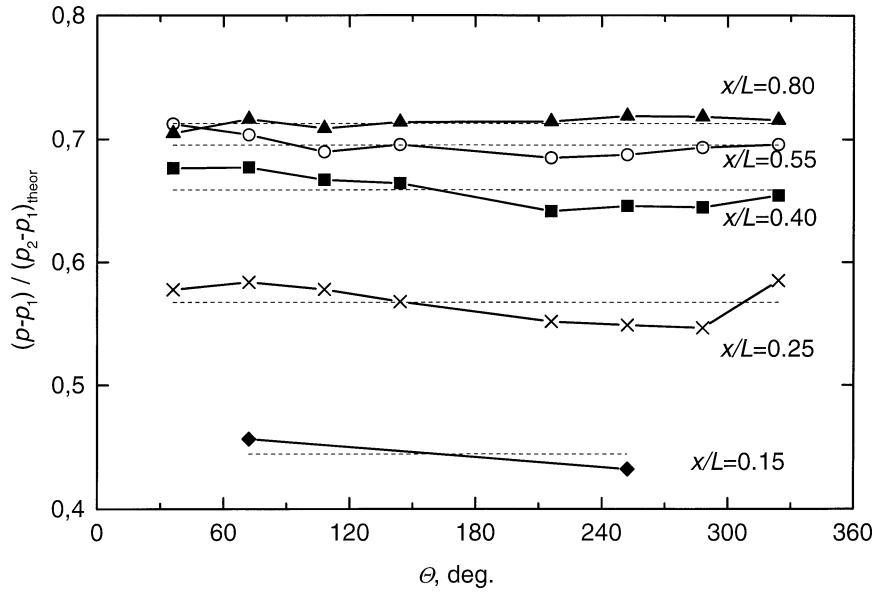

Figure 11. Circumferential variation of the static wall pressure in the 7°-diffuser ($Ma_0 = 0.3$).

the ordinate scales for the 3°-diffuser and the 7°-diffuser differ by 20 dB which is a clear indication of the increase of the unsteady wall pressures due to the flow separation occurring in the latter. A comparison of the azimuthally averaged wall pressure spectra at the different axial locations in the diffusers with the sound pressure spectra at the pipe wall in the acoustic far field is provided in *figure 13*.

In *figure 14* are shown spectra of the coherence between the wall pressures in the diffusers and the sound pressure in the acoustic far field, i.e., at the pipe wall eleven pipe diameters downstream of the nozzle exit ($x/d = 11$). The presentation is similar to that in *figure 12*. The coherence spectra are characterised by a strong frequency dependence with relative maxima occurring at odd multiples of 7.5 Hz, and relative minima at even multiples of 7.5 Hz. This effect is particularly clear in the coherence spectra for the 3°-diffuser and can also be observed in the wall pressure spectra depicted in *figure 12*. At these low frequencies, the anechoic pipe termination is practically inefficient because of its relatively small lateral dimensions; compare *figure 2*. Hence the relative maxima and minima in the coherence spectra can be referred to a longitudinal system resonance: the total length of the test rig, i.e., from the compressor outlet (not shown in *figure 1*) to the end of the anechoic termination is about 11.3 m which equals one-quarter sound wavelength at 7.5 Hz. $\lambda/4$-resonances are generally observed in pipes which are closed at one end and open at the other. In the present test rig, the compressor forms the 'closed' acoustic boundary condition and the anechoic termination, being inefficient at low frequencies, the 'open' end.

Another strong peak in the coherence spectra, and somewhat weaker in the wall pressure spectra and in the far-field spectra (pipe wall at $x/d = 11$), is observed at about 1200 Hz. This peak can be explained by a longitudinal resonance in the diffuser because one half sound wavelength at 1200 Hz equals 0.143 m which corresponds to the length of the diffuser (100 mm) plus some added length of the upstream nozzle plus end corrections; this notion is supported by the observation that the peaks at 1200 Hz are less pronounced near the diffuser exit.

Again, there is a striking difference between the two diffuser angles: the 3°-diffuser shows a fairly axisymmetric behaviour while the scatter of the coherence data for the 7°-diffuser is quite large. At frequencies below 1000 Hz, the coherence with the acoustic far field pressure is much higher in case of the 7°-diffuser

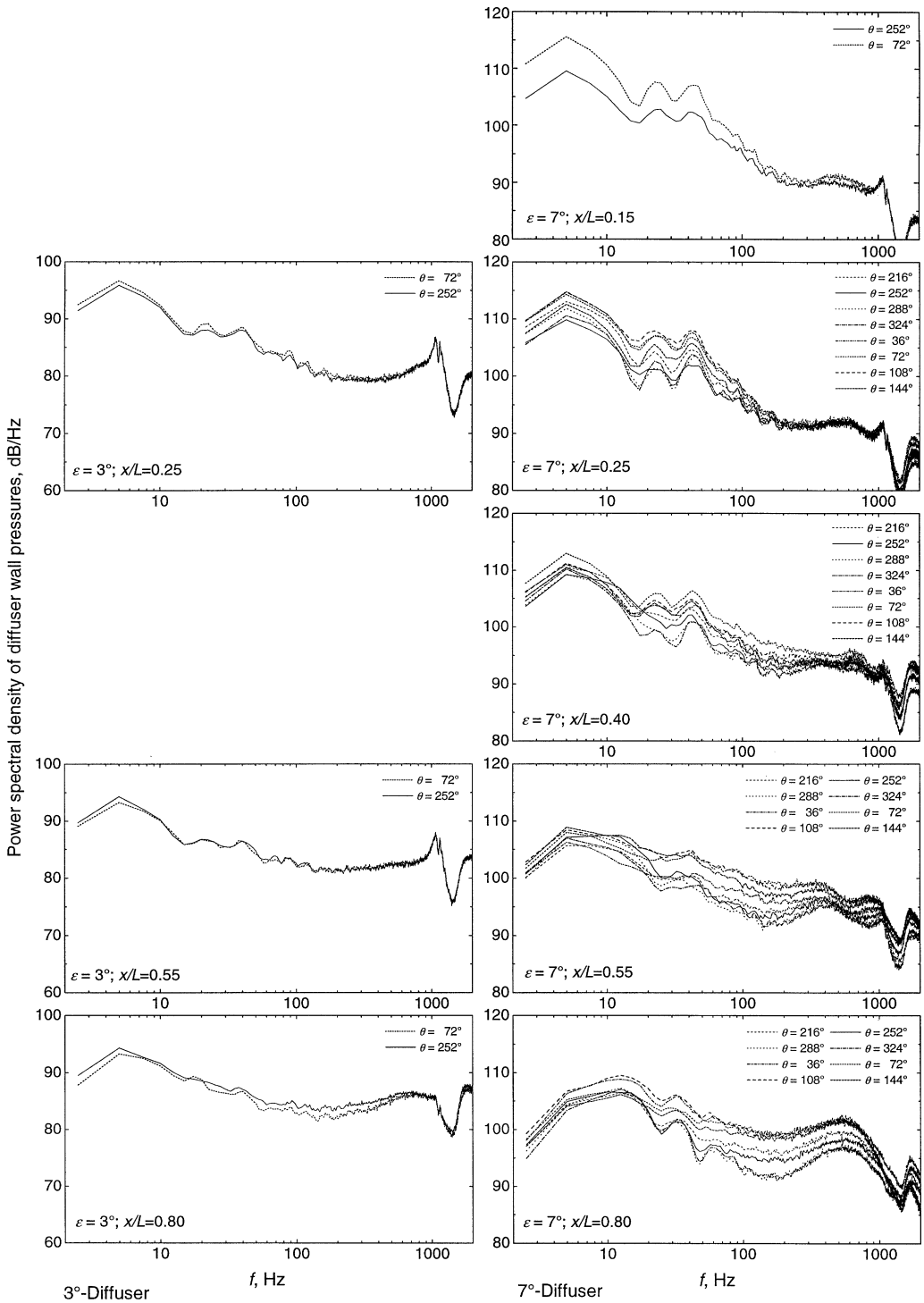

Figure 12. Power spectral density of the diffuser wall pressures.

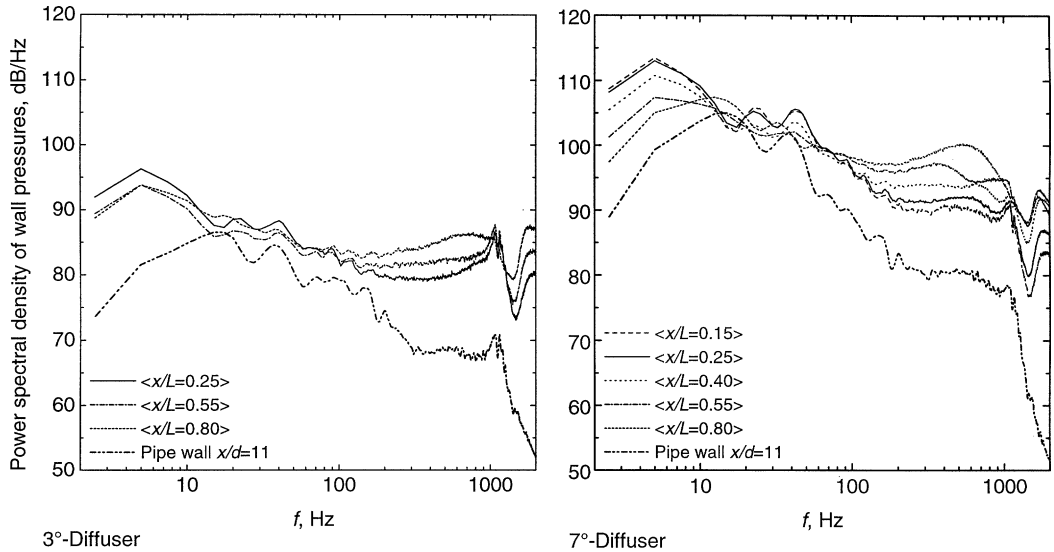

Figure 13. Comparison of azimuthally averaged wall pressure spectra at different axial locations in the diffusers.

which is particularly evident in *figure 15* where the azimuthal averages of the coherence spectra in each axial plane are compared.

The coherence between the wall pressures at different locations within the diffusers is depicted in *figure 16*. The comparison shown is not quite ideal since the reference position is at $x/L = 0.25$ in case of the 3°-diffuser and at $x/L = 0.15$ in case of the 7°-diffuser. Nevertheless it appears that in the frequency range between 300 and 1000 Hz the coherence within the diffuser with the larger expansion angle is distinctly higher than within the smaller angle diffuser. Also, the scatter of the data when different measurement positions are considered for the same reference position is very small for $\varepsilon = 3°$ compared to $\varepsilon = 7°$. The general impression derived from *figure 16* is that the wall pressures in the latter case are more coherent than in the former.

Since the time averaged flow in the 3°-diffuser is axisymmetric as is evident from the wall streamlines (*figure 8*) and the wall pressure spectra (*figure 12*, left column), one might expect coherence values close to 1 in the top left graph of *figure 16* where the coherence is measured between symmetric points MP1 and MP4. This is clearly not the case, at least not for the entire frequency range, and one has to conclude that the fluctuating pressure field inside the 3°-diffuser is not fully coherent across the cross-section and not axisymmetric like in case of a plane sound wave. The pressures measured on the diffuser wall are dominated by the aerodynamic fluctuations of the diffuser flow.

Figure 17 shows the phase of the cross spectra of the wall pressures in the 100 mm diameter pipe ($x/d = 11$) and the wall pressures inside the two diffusers at various axial positions, i.e., at $x/L = 0.25$ (MP4), 0.55 (MP5), and 0.8 (MP6) for the 3°-diffuser and $x/L = 0.15$ (MP1), 0.25 (MP7), 0.4 (MP8), 0.55 (MP9), and 0.8 (MP10) for the 7°-diffuser. The frequency range covered is 0–2000 Hz in the upper graphs and 0–333 Hz in the lower. For the 3°-diffuser as well as the 7°-diffuser, there is a linear drop of the phase angle with frequency over a fairly large frequency range: about 50–1700 Hz for the 3°-diffuser and 200–1500 Hz for the 7°-diffuser. At the low and high frequency ends the phase spectra are less regular than in the medium range.

At low frequencies, the mean gradient of the phase spectra is about the same as in the medium range, but there is a larger scatter, in particular in the 7°-diffuser when measurement points near the exit plane are considered. The scatter of the phase data is most likely due to the fact that the sound waves are superimposed by turbulent pressure fluctuations. It was shown by Stahl [5] that in such a case the resultant phase of the cross spectrum of

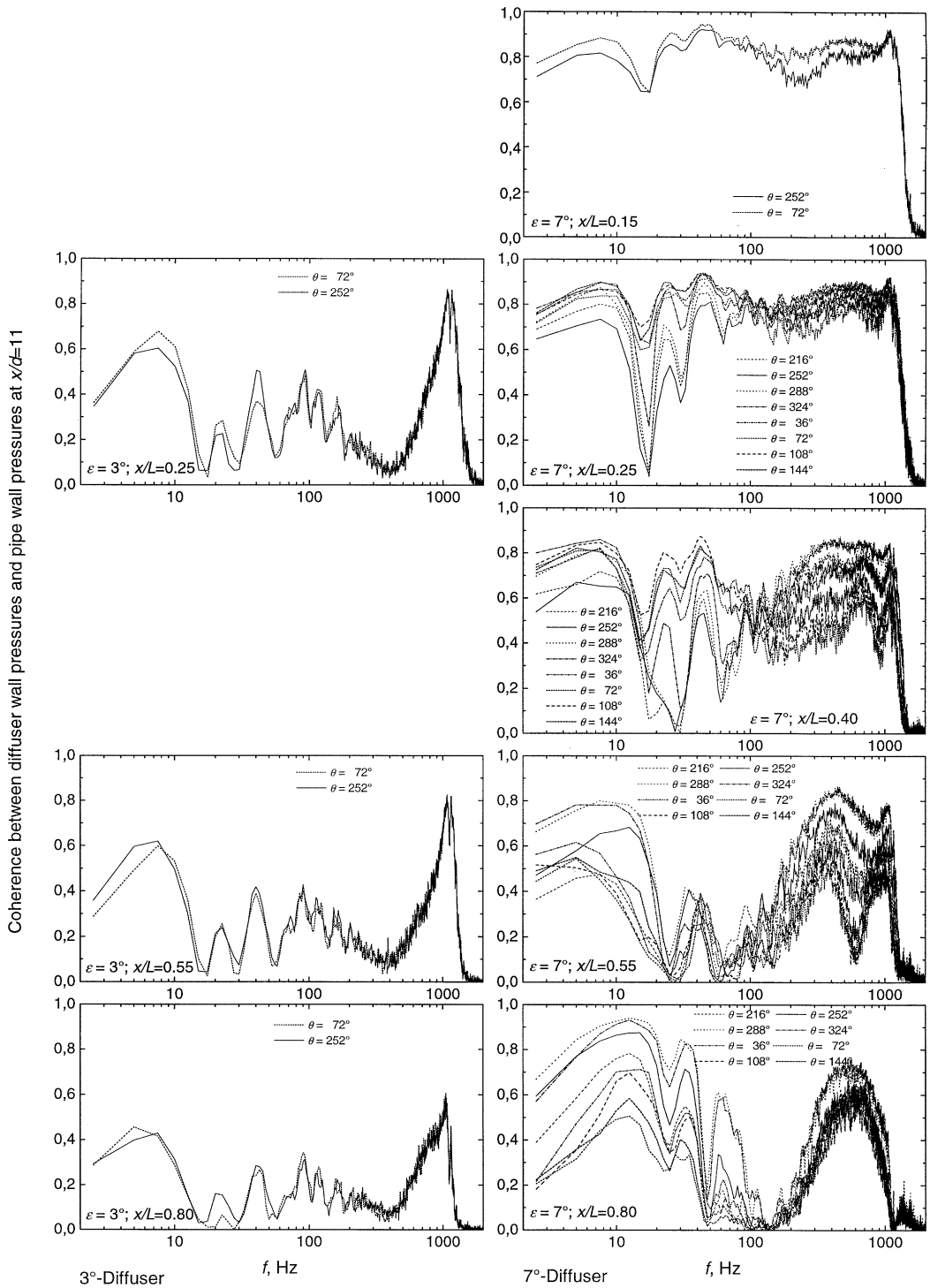

Figure 14. Spectra of the coherence between the wall pressures in the diffuser and in the acoustic far field (pipe wall at $x/d = 11$).

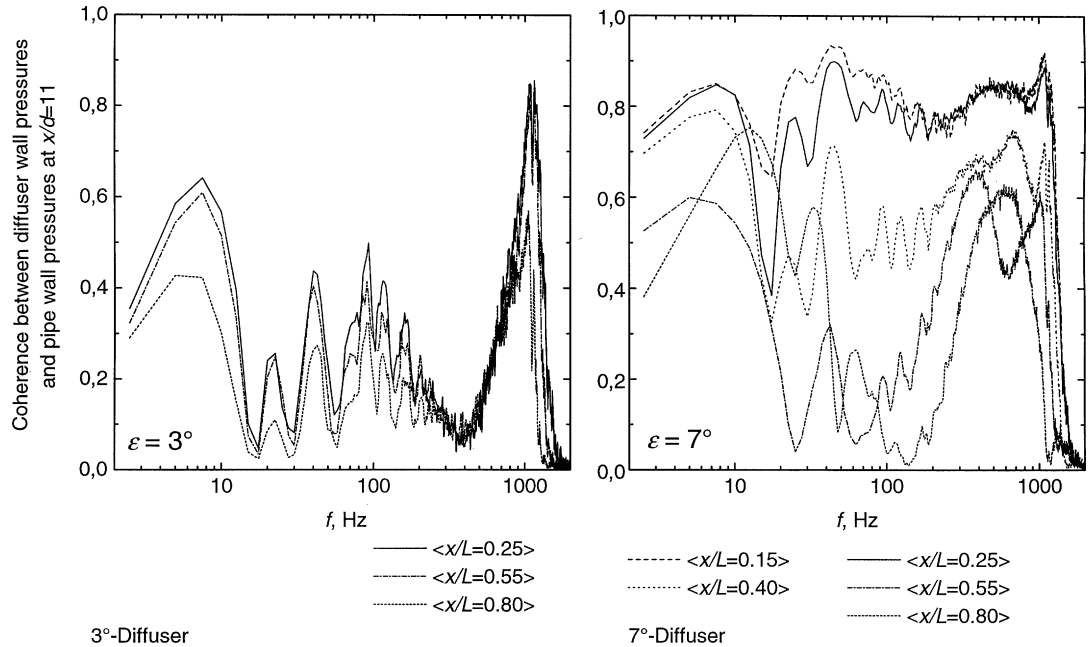

Figure 15. Comparison of azimuthally averaged spectra of the coherence between the wall pressures in the diffuser and in the acoustic far field (pipe wall at $x/d = 11$).

the fluctuating pressures measured at two axially displaced locations is a function of the relative amplitudes of sound and turbulent pressures. Only if one of the two signal components is dominating, is the phase of the cross spectrum a measure of the phase velocity of that component. When sound and turbulent pressure amplitudes are of similar order, the phase spectrum is due to the combined effects of the two pressure components which have different axial phase velocities. This seems to be the case in the 7°-diffuser at frequencies below 150 Hz.

The linear portions of the phase spectra can be used to determine the axial phase velocity of the pressures travelling from the measurement location inside the diffuser to the acoustic far field, using the following considerations (see also Bendat and Piersol [6]): Propagation of a plane sound wave (up to 2010 Hz in a 100 mm diameter duct) can be expressed as follows:

$$p(x,t) = \mathrm{Re}\{A\mathrm{e}^{i(k_x x-\omega t)}\}, \tag{1}$$

where $k_x = 2\pi f/a_x$ is the wave number in the x-direction and a_x the corresponding phase velocity. The phase difference between the sound pressures at two locations x_1 and x_2 at an instant of time ($t = \text{const}$) is given by

$$\varphi_{12} = k_x(x_1 - x_2) = 2\pi f(x_1 - x_2)/a_x. \tag{2}$$

From equation (2) follows for the axial phase velocity for non-dispersive wave propagation

$$a_x = 2\pi(x_1 - x_2)\Big/\frac{\mathrm{d}\varphi_{12}}{\mathrm{d}f}, \tag{3}$$

which shows that the axial phase velocity is proportional to the gradient of the phase angle with respect to frequency. When equation (3) is applied to the frequency range where the phase angle changes linearly

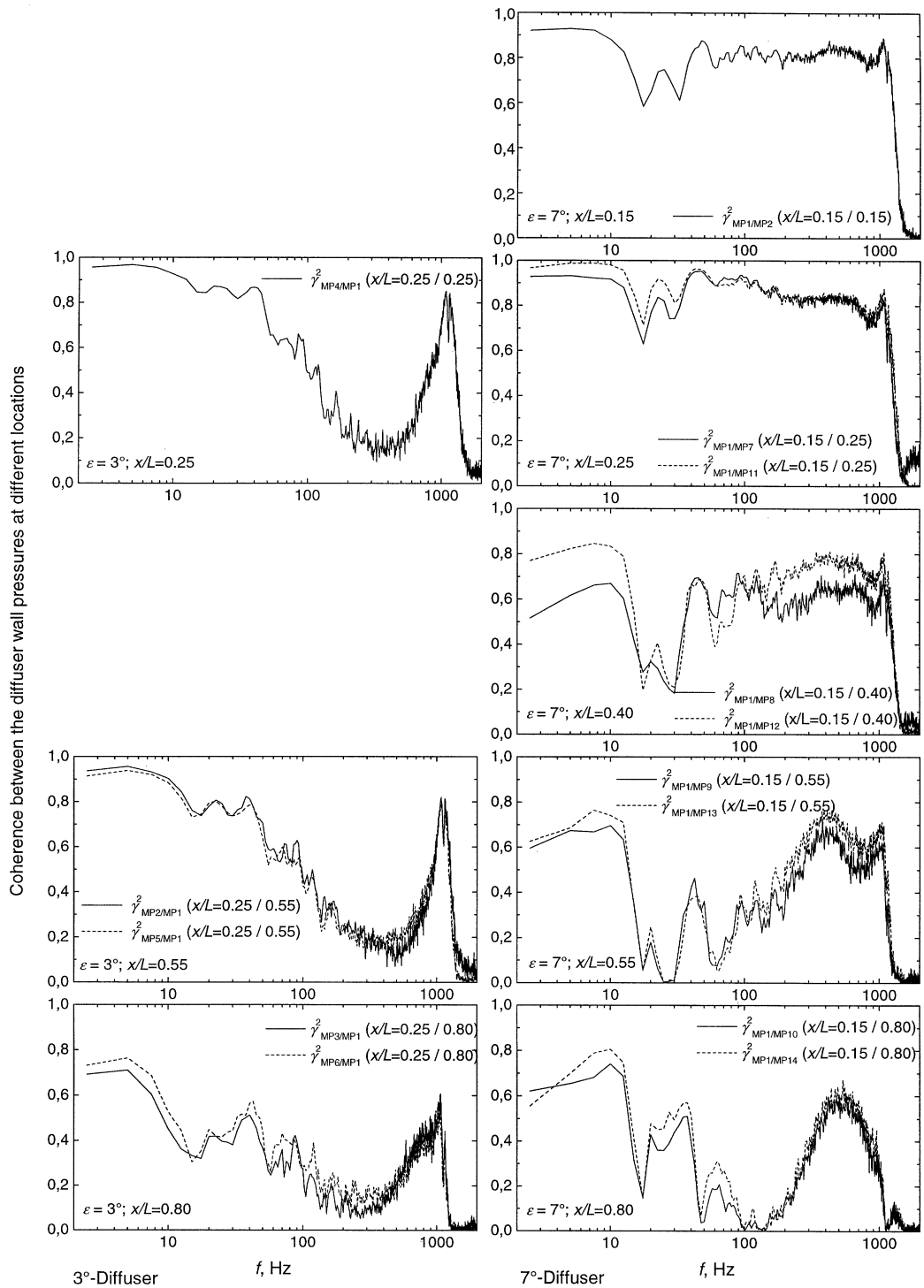

Figure 16. Spectra of the coherence between wall pressures within the diffuser.

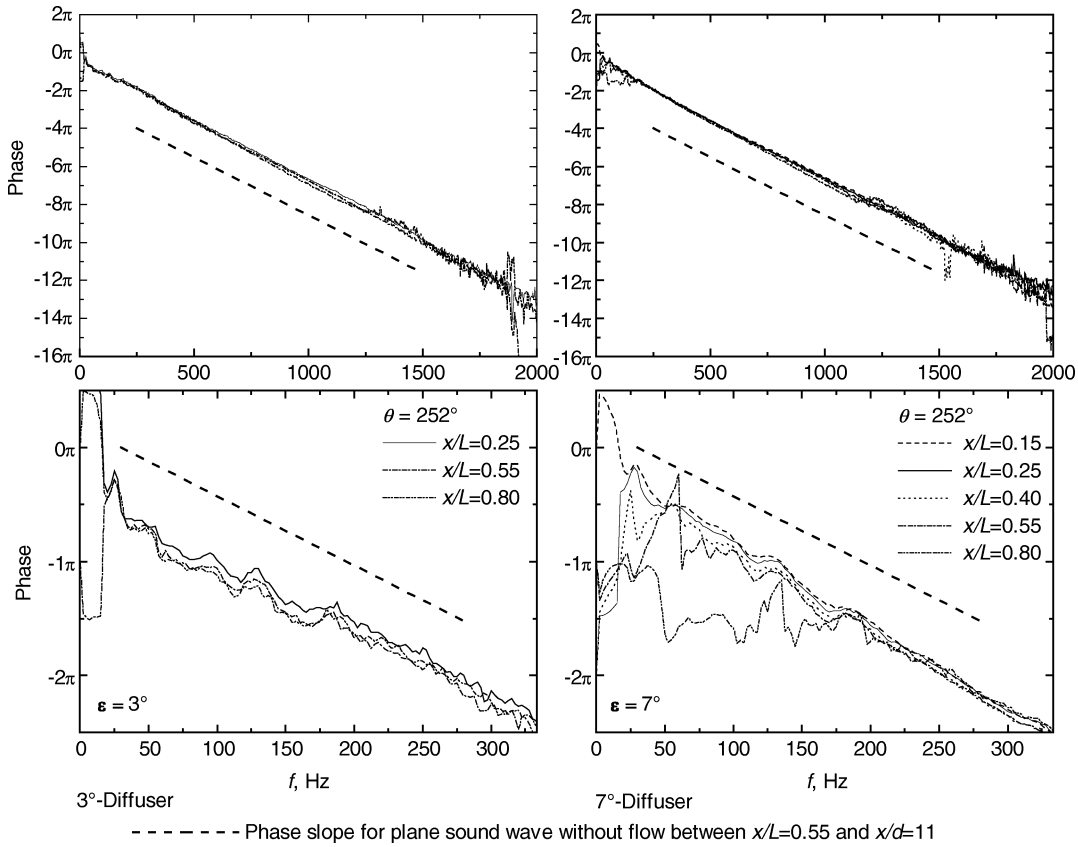

Figure 17. Phase of the cross spectra of the diffuser wall pressures and the sound pressure in the pipe at $x/d = 11$.

with frequency, one obtains axial phase velocities which are equal to the speed of sound, within experimental accuracy, as indicated by the straight lines in the four graphs of *figure 17*. This proves that for both diffusers the sound field in the pipe is generated by the diffuser flow in the respective frequency range. To give an example for the 7°-diffuser, the average axial phase velocity obtained from the phase spectra taken at all eight circumferential measurement points at $x/L = 0.55$ (compare *figure 5*) amounts to 340 m/s.

4. Conclusions

Earlier investigations by Stahl and Argüello [1], who studied the sound field in a circular duct generated by a jet flow, indicated that flow separation occurring in a diffuser attached to the convergent jet nozzle leads to increased sound levels in the low frequency regime. This effect is studied further in the present paper. The experimental rig used is practically the same as that of Stahl and Argüello.

The sound field in a circular duct of $d = 100$ mm diameter is generated by a concentric jet flow entering the pipe at one end. Three cases are compared: In the first case, the air enters through a convergent nozzle, in the second case a diffuser of $L = d$ length and half angle $\varepsilon = 3°$ is attached to the nozzle, and in the third case the diffuser half angle is increased to $\varepsilon = 7°$. The sound field in the pipe is monitored by using a wall-flush mounted microphone at an axial distance of $x/d = 11$ from the exit plane of the convergent nozzle.

Attaching the 3°-diffuser to the nozzle results in a reduction of the sound pressure level in the pipe over the entire frequency range observed (0–12000 Hz, $kR = 0$–11). Increasing the diffuser half angle to 7° further reduces sound levels above 1200 Hz ($kR > 1.1$), however, level increases of as much as 15 dB are observed in the frequency range below. The above observations were also made earlier by Stahl and Argüello [1].

Flow visualization experiments revealed a completely axisymmetric flow pattern of wall streamlines and no indication of flow separation in case of the 3°-diffuser and the existence of a non-axisymmetric flow separation regime in case of the 7°-diffuser, beginning at about 15% of ist axial length and extending over about 85% of the diffuser circumference in the exit plane.

A weak deviation from axisymmetry was also found in the static wall pressure distribution of the 7°-diffuser: the circumferential variation was ±4% from the mean. Spectra of the unsteady wall pressure measured in the 3°-diffuser proved to be independent of the circumferential angle, while in the 7°-diffuser spectral levels differed by as much as 10 dB. Hence, deviation form axisymmetry is much more pronounced in the unsteady wall pressures than in the steady ones.

The spectral wall pressure levels in the 7°-diffusers are roughly 20 dB higher than in the 3°-diffuser which clearly indicates the importance of separated flow for the pressure fluctuations inside the diffuser and the resultant sound radiation into the pipe. Not only are the fluctuating wall pressures more intense when flow separation occurs, but also is the coherence between diffuser wall pressures and acoustic far field pressures higher in this case.

The above experimental results give evidence that flow separation near solid walls is the cause of excess low frequency noise. This statement holds true not only for the diffuser case studied in this paper but also for other flow configurations: It was shown by the present authors [4,7–9] that flow separations along mainly the shroud and the blade suction sides of centrifugal fan impellers are responsible for the low frequency noise emitted by these machines. It was also shown that careful design, in particular of the impeller shroud, can help avoid these low frequency components which are so difficult to diminish once they are generated.

In the diffuser experiment discussed here, flow separation in the 7°-diffuser produces higher sound levels than the free shear layer of the jet flow emanating from the convergent nozzle even though the jet velocity is higher than that in the diffuser. Therefore, as a general rule, flow separation from solid walls should be avoided or reduced as much as possible by suitable design whenever low frequency noise is critical.

References

[1] Stahl B., Argüello G., Schallerzeugung und Schalldämpfung in einer Rohrströmung stromab einer unstetigen Querschnittserweiterung, Acustica 65 (1988) 75–84.
[2] Klein A., Review: Effects of inlet conditions on conical-diffuser performance, J. Fluid. Eng.-T ASME 103 (1981) 250–257.
[3] Cekici N., Experimentelle Untersuchung tieffrequenter Schallentstehungsmechanismen an Diffusoren mit und ohne kritischem Öffnungswinkel, Diplomarbeit an der DLR-Abteilung Turbulenzforschung Berlin und dem Institut für Luft- und Raumfahrt der TU Berlin, 1995.
[4] Fehse K.-R., Experimentelle Untersuchungen zur Entstehung tieffrequenter Druckschwankungen bei Radialventilatoren, Doctoral Dissertation TU Berlin, 1997.
[5] Stahl B., Experimenteller Beitrag zur Schallerzeugung durch die Turbulenz in einer Rohrströmung hinter einer unstetigen Querschnittserweiterung. Deutsches Zentrum für Luft- und Raumfahrt, Köln-Porz, DFVLR-FB 86-06, 1986.
[6] Bendat J.S., Piersol G., Engineering Applications of Correlation and Spectral Analysis, John Wiley and Sons Inc., New York, 1980.
[7] Neise W., Fehse K.-R., Entstehungsursachen tieffrequenter Druckschwankungen bei Radialventilatoren II (Abschlußbericht zum AIF/FLT-Vorhaben Nr. 9351), Forschungsvereinigung für Luft- und Trocknungstechnik e.V., Frankfurt/Main FLT 3/1/78/95, 1995.
[8] Fehse K.-R., Neise W., Generation mechanisms of low-frequency centrifugal fan noise, Proc. 4th AIAA/CEAS Aeroacoustics Conference, 2–4 June 1998, Toulouse, France, ISBN 1-56347-267-8; Paper AIAA/CEAS 98–2370 (1998), 948–958.
[9] Fehse K.-R., Neise W., Generation mechanisms of low-frequency centrifugal fan noise, AIAA J. 37 (1999) 1173–1179.